Cancer & Metabolism

RESEARCH Open Access

Serine starvation suppresses the progression of esophageal cancer by regulating the synthesis of purine nucleotides and NADPH

Hui Jie[1,2], Jing Wei[1], Zhuoling Li[1], Min Yi[2], Xinying Qian[1], Yan Li[1], Chunqi Liu[1], Chuan Li[2], Liang Wang[3], Pengchi Deng[4], Lunxu Liu[2], Xiaobo Cen[3] and Yinglan Zhao[1*]

Abstract

Serine metabolism provides important metabolic intermediates that support the rapid proliferation of tumor cells. However, the role of serine metabolism in esophageal squamous cell carcinoma (ESCC) and the underlying mechanism remains unclear. Here, we show that serine starvation predominantly inhibits ESCC cell proliferation by suppressing purine nucleotides and NADPH synthesis. Mechanistically, serine depletion led to the accumulation of aminoimidazole carboxamide ribonucleoside (AICAR), an intermediate metabolite of de novo purine synthesis, and AMP/ATP ratio. These increases activated 5′-AMP-activated kinase (AMPK), which subsequently inhibited the mTORC1 pathway by phosphorylating Raptor at Ser792. Moreover, serine depletion decreased NADPH level followed by elevated reactive oxygen species (ROS) production and DNA damage, which induced p53-p21 mediated G1 phase cell cycle arrest. Conversely, serine starvation activated transcription factor 4 (ATF4)-mediated robust expression of phosphoserine aminotransferase 1 (*PSAT1*) which in turn promoted compensatory endogenous serine synthesis, thus maintaining ESCC cell survival under serine-limited conditions. Accordingly, serine deprivation combined with PSAT1 inhibition significantly suppressed ESCC tumor growth both in vitro and in vivo. Taken together, our findings demonstrate that serine starvation suppresses the proliferation of ESCC cells by disturbing the synthesis of purine nucleotides and NADPH, and the combination of serine deprivation and PSAT1 inhibition significantly impairs ESCC tumor growth. Our study provides a theoretical basis for targeting serine metabolism as a potential therapeutic strategy for ESCC.

Keywords Serine starvation, ESCC cell proliferation, Purine synthesis, AMPKα / mTORC1 pathway

Introduction

Esophageal cancer ranks as the 11th most commonly diagnosed cancer (511,000 new cases) and is the seventh leading cause of cancer-related deaths (445,000 deaths) worldwide [1]. Esophageal squamous cell carcinoma (ESCC) is the predominant histological subtype of esophageal cancer and exhibits limited sensitivity to chemotherapy or radiotherapy. The esophagectomy is the main curative treatment for ESCC. However, approximately 40% of patients with ESCC are diagnosed with advanced unresectable or metastatic disease, resulting in an overall 5-year survival rate below 40%, which is still far from satisfactory. Moreover, there is no effective targeted

*Correspondence:
Yinglan Zhao
zhaoyinglan@scu.edu.cn
[1] Department of Biotherapy, Cancer Center and State Key Laboratory of Biotherapy, West China Hospital, Sichuan University, Chengdu 610041, China
[2] Department of Thoracic Surgery and Institute of Thoracic Oncology, West China Hospital, Sichuan University, Chengdu 610041, China
[3] National Chengdu Center for Safety Evaluation of Drugs, State Key Laboratory of Biotherapy, West China Hospital, Sichuan University, Chengdu 610041, China
[4] Analytical & Testing Center, Sichuan University, Chengdu 610041, China

drug for ESCC treatment due to the lack of understanding regarding the development of ESCC [2]. Therefore, in-depth study of molecular markers associated with the progression of ESCC and understanding the key pathogenic processes involved is urgent for developing novel therapeutic strategies.

The metabolic reprogramming of tumors provides bioenergy and biosynthesis for the rapid growth of tumor cells and response to survival pressure. In addition to glucose, amino acids play a crucial role by supplying both energy and raw materials that support tumor progression. Among these, the nonessential amino acid serine is the one of the most consumed amino acids in cancer cells [3]. In addition to its role in protein synthesis, serine contributes to the anabolic pathways, which are important for the generation of glutathione, nucleotides, phospholipids and other metabolites [4]. Serine can be converted to glycine by cytoplasmic serine hydroxymethyltransferase 1 (SHMT1) and mitochondrial SHMT2. This reaction yields one-carbon units 5,10-methylene-tetrahydrofolate (5,10-methylene-THF), which enter the THF cycle to form the 10-formyl-tetrahydrofolate (10-formyl-THF) that is required for de novo nucleotide biosynthesis [5, 6]. Therefore, the lack of serine damages folate cycle and inhibits the proliferation of various cancer cells, including breast cancer cells, melanoma cells, and colorectal cancer cells [7–9]. Meanwhile, the synthesis of one-carbon units from serine also leads to the production of NADPH from $NADP^+$. NADPH is important for maintaining cellular redox homeostasis by reducing oxidized glutathione (GSSG) to reduced glutathione (GSH), which scavenges reactive oxygen species (ROS). The inhibition of serine catabolic pathway reduces the cellular NADPH/$NADP^+$ ratio, increases cellular ROS levels, and triggers cancer cell death. In proliferating cells, the oxidative pentose phosphate pathway (PPP) from glucose is traditionally considered the largest contributor to cytosolic NADPH [10]. However, a recent study found that the amount of NADPH derived from serine-driven folate cycle is nearly comparable to that from PPP [11]. Given these findings, we speculate that serine metabolism may play an important role in nucleotide synthesis and redox balance maintenance in ESCC, thus influencing ESCC cell proliferation. However, the role of serine metabolism in ESCC development remains unclear.

mTOR is a central regulator of metabolism and cell proliferation. It functions through two distinct multiprotein complexes, mTORC1 and mTORC2, which are involved in a wide network of signaling pathways [12–14]. The mTORC1 complex consists of mTOR, Raptor, PRAS40 and GβL. This complex mediates the phosphorylation of ribosomal S6 kinase (p70S6K) and 4EBP1, stimulates mRNA translation and acts as a master regulator of cell growth, angiogenesis, and metabolism. mTORC1 can be activated by Rheb-GTP on the surface of lysosomes. The TSC1/TSC2 complex, a small molecule GTPase inhibiting Rheb-GTP, negatively regulates mTORC1 activity [15]. AMPK, an important sensor of cellular energy homeostasis, inhibits mTORC1 signaling by directly phosphorylating Raptor at serine 792 or TSC2 at threonine 1462 [16]. Amino acids such as arginine and leucine regulate mTORC1 signaling by mediating the heterodimer formation of small molecule GTPase Rag family, thus activating mTORC1 on the surface of lysosomes [17–23]. Leucine also activates mTORC1 by recruiting it to the lysosomal surface via GCN2/ATF4/SESN2 signaling pathway [24]. Serine has been implicated in maintaining mTORC1 activity in colorectal cancer [9, 25]. However, the role of serine and mTOR pathway in ESCC cell proliferation remains to be elucidated.

In our study, we demonstrate that serine plays an important role in maintaining the rapid proliferation and redox balance of ESCC cells by participating in purine nucleotide and NADPH synthesis, which subsequently regulates the AMPKα/mTORC1 signaling pathway and p53-p21-mediated G1 phase cell cycle. Meanwhile, the robust expression of *PSAT1* induced by serine depletion in turn promotes compensatory endogenous serine synthesis. Accordingly, serine deprivation combined with PSAT1 inhibition significantly suppresses ESCC tumor growth in vitro and in vivo. In summary, our study provides a theoretical basis for targeting serine metabolism as a potential therapeutic strategy for ESCC.

Materials and methods

Cell lines

Human ESCC cell line KYSE150 was obtained from Shantou University. KYSE180, KYSE510, KYSE410 and TE-1 cells were purchased from Cobioer Biosciences (Nanjing, China). These cell lines were identified by Cell Line Authentication and matched completely (Shanghai Biowing Applied Biotechnology, Shanghai, China). For starvation experiments, "assay media" lacking serine or/and glycine was formulated with MEM (Gibco, NY, USA) supplemented with 10% dialyzed FBS (Wisent, Montreal, Canada), 2 mM L-glutamine (Sigma-Aldrich, MO, USA), 25 mM D-(+)-glucose (Sigma-Aldrich), 1X MEM vitamins (Thermo Scientific, MA, USA). "Complete medium" was formulated with "assay media" supplemented with 0.4 mM L-serine (Sigma-Aldrich) and 0.4 mM glycine (Sigma-Aldrich).

Cell proliferation assay

For cell proliferation assay, cells (1×10^3 cells/well) were seeded into 96-well plates. After 24 h, cells were treated with various concentration of serine and/or glycine for

24–96 h followed by MTT (Sigma-Aldrich) assay. The OD value of each well was measured by a microplate reader (Thermo scientific) at a wavelength of 570 nm.

EdU incorporation assay

EdU incorporation assay was performed by using Cell-Light EdU Apollo567 In Vitro Kit (RIOBIO, Guangzhou, China) according to manufacturer's instructions. Briefly, cells were pulse-labeled with 10 μM 5-ethynyl-2-deoxyuridine (EdU) for 2 h at 37 °C and fixed for 30 min at room temperature with 4% paraformaldehyde. The fixed cells were incubated in glycine solution for 5 min followed by 0.5% Triton X-100 in PBS for 10 min. Then cells were stained with Alexa 567 EdU detection reagent and 1 μg/mL hoechst33342 (100:1). Images were captured by using a High Content Screening Platform (CellInsight CX7, Thermo Scientific). The excitation/emission wavelengths for Apollo567 and hoechst33342 were 550/565 nm and 350/461 nm, respectively.

Cell cycle synchronization and cell cycle analysis

Cells were synchronized in G1/S phase by double-thymidine block. KYSE150 and KYSE180 cells (2×10^3 cells/well) were seeded in 6-well plates and allowed to adhere for 24 h, then treated with 2 mM thymidine (Sigma-Aldrich) for 16 h followed by releasing for 10 h. Then cells were treated with 2 mM thymidine again for 16 h followed by releasing in media with or without serine. After specified time points, cells were fixed in pre-cooled 75% ethanol, incubated with propidium iodide (PI) (Sigma-Aldrich) solution (50 μg/mL PI, 100 μg/mL RNase A, 0.1% Triton X-100 in PBS) for 10 min. Cell cycle was detected by using Cytomics FC 500 (Beckman Coulter, CA, USA) and data was analyzed by Flow Jo 10.0 (Leonard Herzenberg, USA).

RNA isolation and quantitative real-time reverse-transcription polymerase chain reaction (RT-qPCR)

RNA was extracted from cells and tissues using Multi-source Total RNA Mini Kit (Axygen Scientific, CA, USA) and reverse transcription was accomplished with RevertAid First Strand cDNA Synthesis Kit (Thermo Scientific) according to the manufacturer's instructions. qPCR was performed using an Applied Biosystems CFX96 Fast Real-Time PCR system (Bio-Rad, CA, USA) with SsoAdvanced™ Universal SYBR Green Supermix (Bio-Rad). Expression results obtained were normalized to *ACTB* levels and triplicate assays were performed. Solubility curves were analyzed to exclude the possibility of nonspecific amplification products. Primer sequences were listed in supplementary Table S1. Sequences were synthesized and purified by Shanghai Sangon Biotech (Shanghai, China).

Immunoblotting and antibodies

For protein analysis, cells were treated with or without serine for a period of time and lysed on ice in RIPA buffer (Beyotime, Shanghai, China) containing protease inhibitors (Selleck, Houston, USA) for 30 min. The crude lysates were centrifuged at 13,300 rpm for 15 min at 4 °C. The supernatants were collected and protein concentrations were determined by Coomassie brilliant blue G250 (Bio-Rad). Protein loading buffer (Beyotime, Shanghai, China) was added to cleared lysates which were subsequently boiled for 5 min. Samples were loaded into SDS-polyacrylamide gels (Bio-Rad), resolved by electrophoresis, transferred onto polyvinylidene fluoride membranes (Millipore, MA, USA), and probed using the indicated antibodies. Protein bands were visualized with the chemiluminescence imaging system (CLINX, shanghai, China) using chemiluminescent HRP substrate ECL (Millipore).

The following antibodies for immunoblotting were purchased from Cell Signaling Technology (CST): p-AMPKα (Thr172) (#8208), AMPKα (#5831), p-Raptor (Ser792) (#2083), Raptor (#48648), p-p70S6K(Thr421/Ser424) (#9204), p70S6K (#9202), p-S6(Ser235/236) (#4858), S6 (#2317), p-mTOR (Ser2448) (#5536), mTOR (#2983), p-p53(Ser15) (#82530), p21(#2947), and PHGDH (#66350). PSAT1 antibody was obtained from Proteintech Group (67619–1-Ig). PSPH antibody was from Novus (NBP1-56848). p53 antibody (sc-126) was obtained from Santa Cruz Biotechnology. β-actin (BM3873), HRP-labeled goat anti-rabbit (BA1054) and goat anti-mouse (BA1056) secondary antibody were obtained from Boster (Wuhan, China).

Nontarget metabolomics profiling based on UPLC/Q-TOF–MS/MS

The metabolites of intracellular water phase were analyzed by UPLC/Q-TOF–MS/MS according to previous report [1]. Briefly, cells ($3–4\times10^5$ cells/well) were seeded in 6-well plates. After 24 h, cells were washed with PBS, and 2 mL assay media with or without serine was added for 24 h. Metabolites were extracted by lysing cells in ice-cold methanol/acetonitrile/H_2O (50:30:20). Samples were shaken at 4 °C for 10 min, then centrifuged for 15 min at 16,000 g, and the supernatant was collected and dried by nitrogen blower. The dried metabolites were resuspended in water and centrifuged at 13,000 g at 4 °C for 10 min, and the supernatants were collected for metabolite analysis.

Metabolites were separated using hydrophilic interaction liquid chromatography with an Acquity UPLC BEH HILIC column (2.1 × 100 mm, 1.8 μm) (Waters, USA) and detected with UPLC/Q-TOF–MS/MS (XevoG2-sQ-TOF,

Waters). Column compartment was set to 35 °C, and autosampler sample tray was set to 4 °C. The elution buffers were acetonitrile for buffer A and 20 mM $(NH_4)_2CO_3$ and 0.1% NH_4OH in H_2O for buffer B. A linear gradient was programmed starting from 80% buffer A and ending at 20% buffer A after 20 min, followed by wash (20% buffer A) and re-equilibration (80% buffer A) steps with a flow rate of 100 mL/min. The mass spectrometer was fitted with an electrospray-ionization probe and operated in full-scan and polar-switching mode with the positive voltage at 4.5 kV and negative voltage at 3.5 kV.

The analysis of intracellular metabolites was performed as previous report [2]. Briefly, metabolite identification and data analysis were carried out using the Progenesis QI software (Newcastle, UK) and EZinfo software. Metabolites were identified by referring to the Lipid Maps Database (www.lipidmaps.org) and the Human Metabolome Database (http://www.hmdb.ca/). Metabolites with the highest impact on the group clustering were identified in the variable importance (VIP)-plots (VIP > 1). Besides, unpaired Student's t-test ($p < 0.05$) to the chemical shifts was used to assess the significance of each metabolite. The metabolites in two groups which showed both VIP > 1 and $P < 0.05$ were identified as significant difference. Plotted values are normalized to endogenous metabolites. Enrichment of metabolic pathways was carried on with the Metabo Analyst website (https://www.metaboanalyst.ca).

Target metabolomics profiling

KYSE150 cells grown in Com or -Ser medium for 24 h were harvested with 0.25% trypsin and adjusted to a density of $4*10^6$ cells/well. Metabolites were extracted by lysing cells in ice-cold methanol/H_2O (80:20). Samples were shaken at 4 °C for 15 min, then centrifuged for 10 min at 13,000 g, and the supernatant was collected and completely dried by conduct vacuum centrifugation at 30℃ for 6 h. The dried metabolites were resuspended in 0.6 mL of HILIC solution with 13C1-Lactate (as an internal standard), vortexed at 4 °C for 30 min, and centrifuged at 13,000 g at 4 °C for 10 min. The supernatants were analyzed by LC–MS (AB Sciex6500). Plotted values are normalized to 13C1-Lactate.

Gene silencing

siRNA for knockdown of *PRKAA1, ATF4* and control siRNA were purchased from RIOBIO (Guangzhou, China). KYSE150 and KYSE180 cells were transfected using Lipo2000 (Thermo Scientific) according to the manufacturer's instruction. siRNA interference sequences are shown as follows: si*ATF4*#1 GAAGGA GTTCGACTTGGAT, si*ATF4*#2 GTTGGATGACAC TTGTGAT, si*PRKAA1*#1 GTGGAACCCTTCCATTTG A, si*PRKAA1*#3 GATCCATCATATAGTTCAA and siNC GGAGAGUUGUGGACUUUAU.

The lentiviral package shRNA vector is pLKD-CMV-Puro-U6-shRNA. The sequences targeting *PSAT1* and control (NC) were GCACTCAGTGTTGTTAGAGAT and TTCTCCGAACGTGTCACGT, respectively. The design of above plasmids and lentiviral packaging were completed by Shanghai Heyuan Biotechnology (Shanghai, China). KYSE150 and KYSE180 cells were seeded in 6-well plates at 2×10^5 cells/well. The medium was changed to serum-free medium the next day for infection. A certain volume of virus and polybrene were added according to the viral titer and the complex MOI value of cell infection. After 24 h, the cells were cultured in fresh medium containing 10% FBS for 24 h followed by screening with 2 μg/mL puromycin for 48 h. The interference efficiency was verified by RT-qPCR and immunoblotting.

mRNA sequencing

mRNA sequencing and quality checks was conducted by a profiler service provided by HuaDa Gene Information Technology (Shenzhen, China). Briefly, KYSE150 cells (2×10^5 cells/well) were seeded in 6-well plates, followed by serine-deficient medium treatment for 24 h. Then, cells were collected and total RNA was purified and stored in TRIzol (Invitrogen, USA). Triplicate samples were harvested for each group, and significant probe sets were filtered for detection using a fold-change > 1.5, $P < 0.05$ (Student's t-test) and FDR (false discovery rate) < 0.05. The differentially expressed genes were enriched in Gene Ontology (GO) and Kyoto Encyclopedia of Genes and Genomes (KEGG).

Chromatin immunoprecipitation (ChIP) assay

ChIP assay was performed using EZ-Magna ChIP™ A/G Chromatin Immunoprecipitation Kit (Millipore) according to the manufacturer's instruction. Briefly, cells were treated in complete or serine-deficient media for 24 h. Then cells were fixed with 1% formaldehyde, and cross-linked chromatin was sonicated to produce 200–1000 bp DNA fragments. Chromatin from ~ 1.5×10^6 cells were incubated overnight at 4 °C with 2–5 μg anti-ATF4 antibodies and pre-blocked Protein A/G Plus beads. Normal rabbit IgG was used as control. Then, the protein/DNA complexes were eluted according to the instructions. Free DNA was purified and amplified by qPCR using primers shown in supplementary Table S2.

Tumor xenograft mouse model

ESCC tumor xenograft mouse models were established by subcutaneously injecting vector control or shPSAT1 KYSE150 cells (5×10^6 cells) into the left and right hind flank region of five weeks old nude female mice (HFK

Biotechnology, Beijing China), respectively. Following injection, mice were randomly placed either on control diet (Com) ($n=6$), serine-deficient diet (-Ser) ($n=6$), or serine and glycine-deficient diet (-SG) ($n=6$) (HFK Biotechnology, Beijing, China) and the component of diet was listed in Table S3 [26]. Tumor sizes and animal weight were monitored every 3 days, and volumes were calculated according to the following formula: $L \times W^2 \times 0.5$, where L is the length and W is the width. Mice were sacrificed and tumors were dissected and photographed by camera when tumors reached clinical endpoint of predetermined size.

Statistical analyses

All data are represented as mean ± SD. Data were collected in Microsoft Excel (v.12.3.6) and all statistical analyses were performed using GraphPad Prism 9 (Graph Pad Software, USA). Unpaired/paired Student's t test was performed to compare two groups to each other. If the variance between the two groups was unequal, a Welch's correction was applied. To compare more than two groups, statistical significance was determined using one/two-way ANOVA with Tukey's post hoc test. Statistical significance is indicated as follows: $^{*}p<0.05$, $^{**}p<0.01$, $^{***}p<0.001$, $^{****}p<0.0001$, and $p>0.05$ was considered not significance (ns).

Results

Serine starvation inhibits proliferation and induces G1 phase cell cycle arrest in ESCC cells

To evaluate the role of serine in human ESCC cell proliferation, we detected the ESCC cell proliferation after cultured with formulated media that contained 0.4 mM serine and 0.4 mM glycine (Com), lacking serine (-Ser), lacking glycine (-Gly), or lacking serine and glycine (-SG) for 24—96 h, respectively [9]. MTT assay showed that both -Ser and -SG media significantly decreased the proliferation of KYSE150, KYSE180, KYSE510, KYSE410, and TE-1 cells in a time-dependent manner, whereas -Gly medium had no significant effect (Fig. 1A). This is not surprising, as glycine can be converted from serine through SHMT1/2 when exogenous glycine is deprived. The cell counts are consistent with these findings in KYSE150 and KYSE180 cells (Fig. S1A). Given the notable efficacy of KYSE150 and KYSE180 cells, we chose these cells for subsequent research.

Then, we detected ESCC cell proliferation under various concentrations of serine supplementation. We observed significant inhibition of ESCC cell proliferation in a serine concentration-dependent manner, particularly when serine concentration was below 50 μM (Fig. 1B). The maximum growth inhibition of KYSE150 and KYSE180 cells was 40% and 45% after serine starvation, respectively. Colony formation assays showed that both KYSE150 and KYSE180 cells decreased the number of generated colonies in -Ser medium compared with Com medium (Fig. S1B). Moreover, the death of cells showed no significant change under this condition (Fig. 1C). These results demonstrate that serine starvation inhibits the proliferation of ESCC cells without inducing cell death.

We then analyzed the cell cycle using flow cytometry after serine starvation. After synchronizated in G0/G1 phase by a double-thymidine block, ESCC cells were simultaneously released into Com or -Ser media for a period of time, followed by cell cycle analysis. The results showed that KYSE150 cells had significant G1 phase cell cycle arrest under serine starvation, which was moderate in KYSE180 cells, and both cells eventually recovered integral cell cycle (Fig. 1D, S1C). Furthermore, EdU incorporation assay showed that the number of EdU-positive cells in KYSE150 and KYSE180 cells was significantly reduced by 95% and 73% compared with the control, respectively, suggesting that serine starvation dramatically inhibited DNA synthesis (Fig. 1E). Collectively, these findings indicate that serine starvation inhibits ESCC cell proliferation and induces G1 phase cell cycle arrest.

Serine starvation decreases the purine nucleotide pool by reducing de novo purine synthesis and adenine salvage synthesis

To explore the potential mechanism by which serine deprivation inhibits cell proliferation and impairs DNA synthesis, we performed a nontargeted metabolomics assay on KYSE150 cells after serine starvation for 24 h. A total of 2,211 metabolites were detected in both positive and negative ionization modes (Table S4). Among these, 89 metabolites were identified as significantly altered, with 64 aqueous metabolites visualized in a heat map (Fig. 2A). KEGG pathway enrichment analysis revealed that the differential metabolites were involved in some pathways, including purine metabolism, arachidonic acid metabolism, nicotinate and nicotinamide metabolism (Fig. 2B).

Serine can be converted to glycine by SHMT1/2, a reaction that yields 5,10-methylene-THF, a one-carbon unit involved in the thymidylate synthesis pathway. Despite serine starvation, the levels of glycine and key intermediates of this pathway—thymidine monophosphate (dTMP) and thymidine 5'-triphosphate (dTTP)— were maintained at relatively constant levels (Fig. 2C, S2A). Additionally, 5,10-methylene-THF enters the THF cycle to form 10-formyl-THF, which is required for de novo purine synthesis, and 5-methyltetrahydrofolate (5-methyl-THF), which regenerates

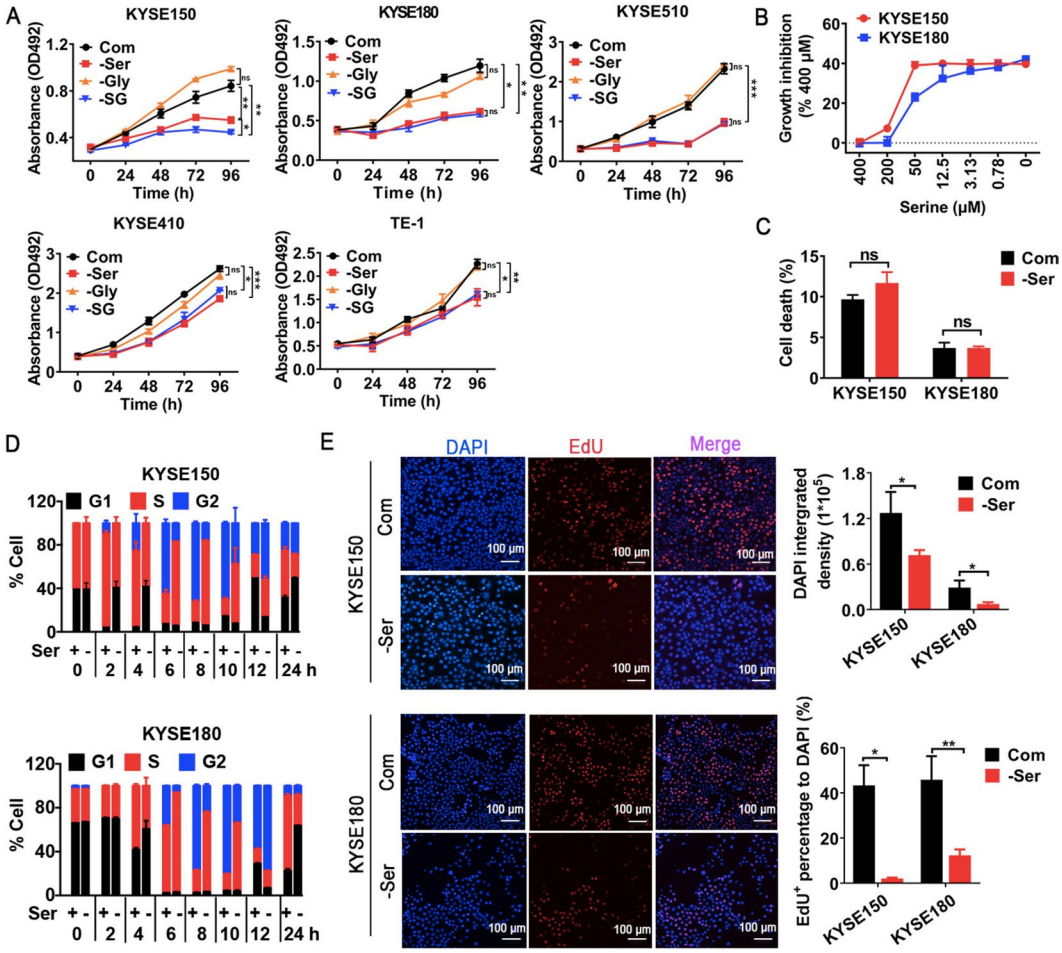

Fig. 1 Serine starvation inhibits proliferation and induces G1 phase cell cycle arrest in ESCC cells. **A** Proliferation curves of ESCC cells grown in Com, -Ser, -Gly or -SG medium. **B** The growth of ESCC cells cultured in indicated concentration of serine was determined by using MTT assay. **C** The mortality of ESCC cells treated in Com or -Ser medium for 24 h was detected by using trypan blue staining. **D** Cell cycle distribution in ESCC cells. The ESCC cells were synchronized and arrested in G0/G1 phase by a double-thymidine block, then simultaneously released in media with or without serine for indicated time, followed by flow cytometry. **E** Representative immunofluorescence images (left) and quantification (right) of EdU incorporation assay in ESCC cells cultured in Com or -Ser medium for 24 h. DAPI was used to stain nucleus. Scale bar represents 100 μm. Data are presented as mean ± SD. Two-way ANOVA with Tukey's post hoc test (**A**) and unpaired two-sided Student's t test (**C** and **E**). ns: no significance, $^{*}p < 0.05$, $^{**}p < 0.01$, $^{***}p < 0.001$

methionine from homocysteine. Unexpectedly, levels of 5-methyl-THF, homocysteine, and methionine remained unchanged in response to serine starvation (Fig. 2C). Moreover, 5-methyl-THF supplementation failed to rescue the proliferation inhibition caused by serine starvation in KYSE150 cells (Fig. S2B). These findings suggest that serine starvation inhibits ESCC cell proliferation through mechanisms independent of the thymidylate synthesis and methionine regeneration pathways.

Meanwhile, the accumulation of glycinamide ribonucleotide (GAR) and AICAR, upstream intermediates of 10-formyl-THF incorporation preceding inosine monophosphate (IMP) in de novo purine biosynthesis, were observed in ESCC cells following serine deprivation (Fig. 2D). These substrates accumulation likely results from decreased level of 10-formyl-THF, which may hinder the purine synthesis. To further investigate the role of purine synthesis in ESCC cell proliferative inhibition induced by serine starvation, we replenished the one-carbon pool by adding 1 mM formate (FA), a substitute of 10-formyl-THF [27], into -Ser medium, and performed cell proliferation, cell cycle, and EdU incorporation assays. The results showed that FA significantly rescued the inhibition of ESCC cell proliferation caused by serine starvation (Fig. 2E). Consistently, FA also reversed G1 phase cell cycle arrest (Fig. S3A) and restored DNA synthesis (Fig. S3B). These results

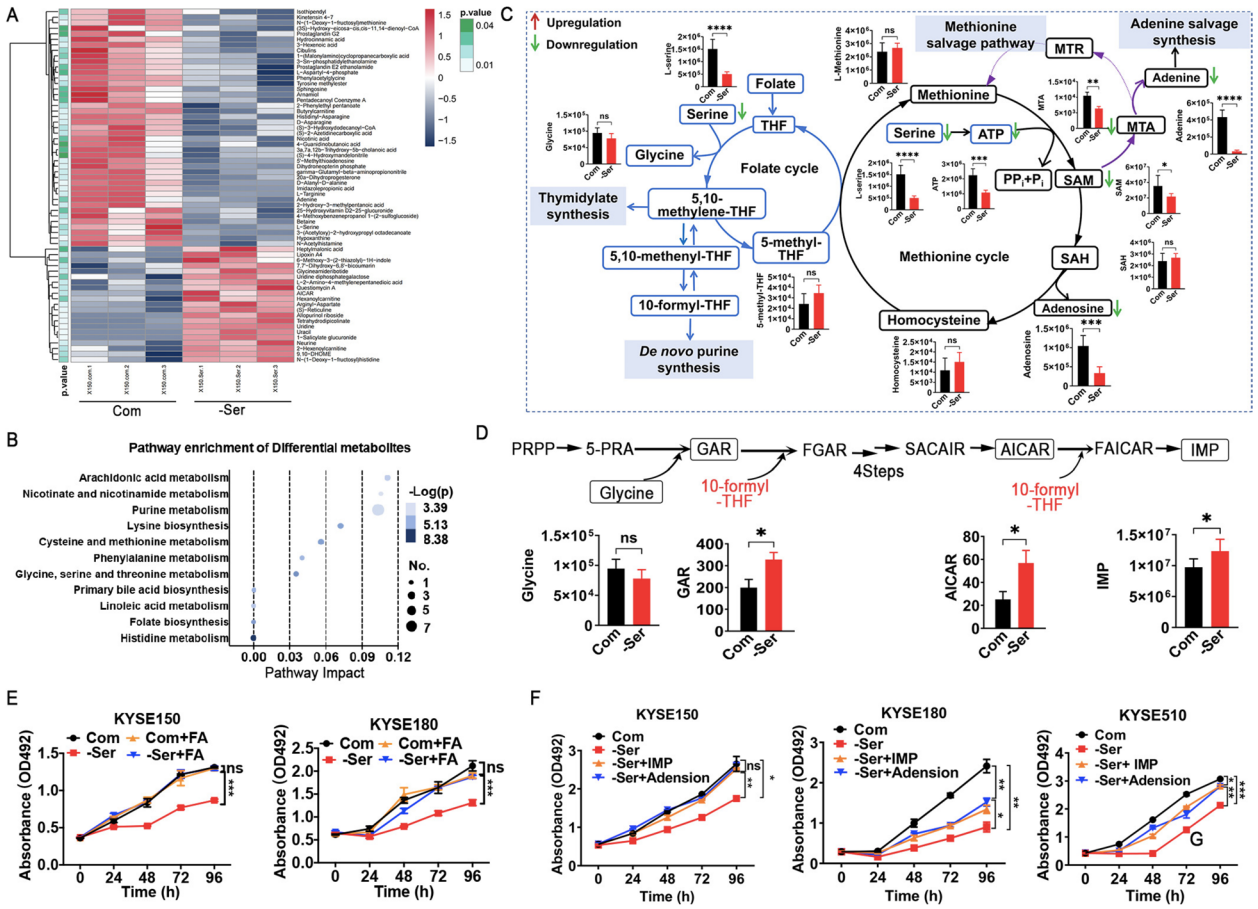

Fig. 2 Serine starvation decreases purine nucleotide pool by reducing de novo purine synthesis and adenine salvage synthesis. **A** The heat map of 64 aqueous metabolites in KYSE150 cells cultured in Com or -Ser medium for 24 h were detected by using a nontargeted metabolomics approach ($n=6$ per group). Data normalized by mean value of Com group. **B** Pathway enrichment analysis of differential metabolites using metabo analyst web. **C** The intermediates of folate cycle and methionine cycle in KYSE150 cells after serine starvation for 24 h were detected by using a targeted metabolomics approach ($n=6$ per group). THF, tetrahydrofolate; SAM, S-adenosyl methionine; MTA, methylthioadenosine; SAH, S-adenosylhomocysteine. **D** The intermediates of de novo purine nucleotide synthesis in KYSE150 cells after serine starvation for 24 h ($n=6$ per group). GAR and AICAR were measured by nontargeted metabolomics approach. Glycine and IMP were measured by targeted metabolomics approach. PRPP, phosphoribosyl diphosphate; 5-PRA, 5-phosphoribosylamine; GAR, glycinamide ribonucleotide; FGAR, glycineamideribotide formylglycinamide ribonucleotide; SAICAR, 4-(N succinylcarboxamide)-5-aminoimidazole ribonucleotide; AICAR, aminoimidazole carboxamide ribonucleoside; FAICAR, formylaminoimidazole-4-carboxamide ribonucleotide; IMP, inosine 5′-monophosphate. **E** Proliferation curves of ESCC cells grown in Com or -Ser medium with the supplementation of 1mM FA. (F) Proliferation curves of ESCC cells grown in Com or -Ser medium with the supplementation of 1mM IMP or adenosine. Data are presented as mean ± SD. Unpaired two-sided Student's *t* test (C and D), and two-way ANOVA with Tukey's post hoc test (E and F). ns: no significance, $*p<0.05$, $**p<0.01$, $***p<0.001$, $****p<0.0001$

suggest that serine supports ESCC cell proliferation through de novo purine synthesis, likely mediated by 10-formyl-THF.

Previous research has reported that serine maintains the methionine cycle through de novo ATP synthesis, supporting the conversion of methionine to S-adenosyl methionine (SAM) [28]. Our results showed that serine starvation led to decreased levels of ATP and SAM, followed by reductions in methylthioadenosine (MTA, an intermediate metabolite involved in the methionine salvage pathway), adenine, and adenosine (Fig. 2C). The replenishment of the purine nucleotide pool by adding IMP or adenosine partially rescued the serine starvation-induced proliferation inhibition (Fig. 2F). These results suggest that serine starvation may reduce the production of adenine and adenosine derived from SAM, thereby impairing adenine salvage synthesis. Meanwhile, the levels of guanosine monophosphate (GMP) and IMP moderately increased, while hypoxanthine and guanosine were dramatically decreased by serine starvation (Fig. S3C), suggesting that the purine salvage pathway for hypoxanthine and guanosine may be compensatorily

activated. Taken together, these data indicate that serine starvation significantly decreases purine nucleotide pool by reducing de novo purine synthesis and adenine salvage synthesis. Restoring the purine pool rescues the proliferation inhibition of ESCC cells induced by serine starvation.

Serine starvation induces AMPKα activation to inhibit mTORC1 signaling pathway

Given that serine starvation led to the increases of AICAR (an AMPK activator) (Fig. 2D) and AMP/ATP ratio (Fig. 3A), we investigated the activation of AMPKα in ESCC cells after serine starvation using western blotting as AMPK is an energy sensor activated by depletion of cellular energy levels. The result showed that the phosphorylation of AMPKα at Thr172 was significantly upregulated in ESCC cells after serine starvation, indicating the activation of AMPKα (Fig. 3B).

Since mTORC1 pathway is the important downstream of AMPK [25], we evaluated mTORC1 activity after serine starvation in ESCC cells. The levels of phospho-p70S6K and phospho-S6, downstream effectors of mTORC1, were downregulated after serine starvation (Fig. 3B). Furthermore, the phosphorylation of Raptor at Ser792 increased, while mTOR phosphorylation at Ser2448 remained unchanged (Fig. 3B). As expected, FA supplementation attenuated the upregulation of p-AMPKα (Thr172) and p-Raptor (Ser792) and restored the downregulation of p-p70S6K and p-S6 induced by serine starvation (Fig. 3C). These results suggest that serine starvation triggers AMPKα activation and mTORC1 signaling inhibition by increasing AICAR level and AMP/ATP ratio.

To further confirm whether serine starvation-induced inhibition of mTORC1 activity is directly mediated by AMPKα, we silenced *PRKAA1* (encoding AMPKα) using siRNA #1 (> 90% depletion compared with the control; Fig. 3D) or inhibited AMPKα by compound C. The results showed that both compound C and si*PRKAA1* rescued the downregulation of

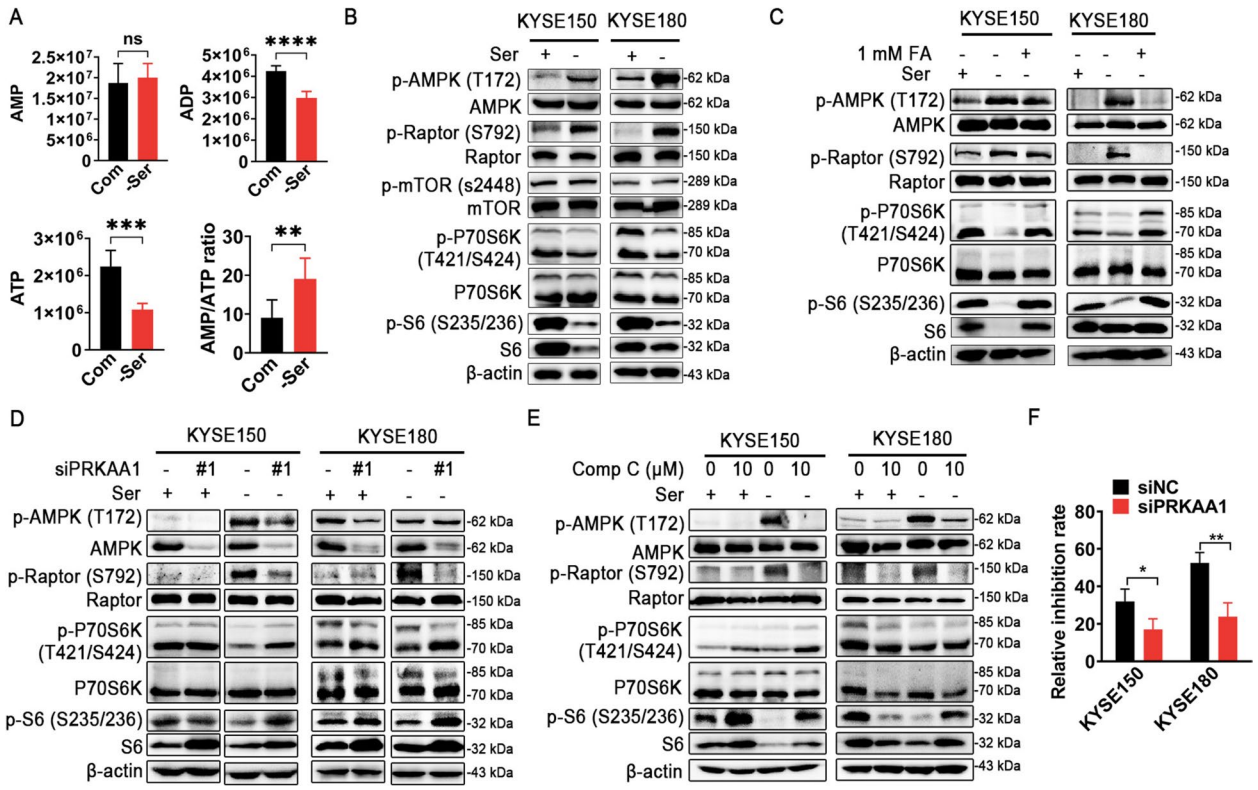

Fig. 3 Serine starvation induces AMPKα activation to inhibit mTORC1 signaling pathway. **A** The levels of AMP, ADP, ATP, and AMP/ADP ratio in KYSE150 cells after serine starvation for 24 h were detected by using a targeted metabolomics approach ($n = 6$ per group). **B**, **C** The levels of AMPKα/mTORC1 signaling pathway in ESCC cells grown in Com or -Ser medium with the supplementation of 1 mM FA for 24 h were detected by western blotting. β – actin was the loading control. **D** The levels of AMPKα/mTORC1 signaling pathway in si*PRKAA1* ESCC cells grown in Com or -Ser medium for 24 h were detected by western blotting. β – actin was the loading control. **E** The levels of AMPKα/mTORC1 signaling pathway in ESCC cells grown in Com or -Ser medium with or not 10 μM compound C for 2 h were detected by western blotting. β – actin was the loading control. **F** The number of si*PRKAA1* ESCC cells grown in Com or -Ser medium for 48 h. Data are presented as mean ± SD. Unpaired two-sided Student's *t* test. ns: no significance, *$p < 0.05$, **$p < 0.01$, ***$p < 0.001$, ****$p < 0.0001$

p-p70S6K and p-S6 and attenuated the upregulation of p-AMPKα (Thr172) and p-Raptor (Ser792) induced by serine deprivation (Fig. 3D, E). Moreover, proliferation inhibition caused by serine starvation was partially restored by *siPRKAA1* in ESCC cells (Fig. 3F). These results suggest that AMPKα plays a crucial role in mediating the inhibitory effects of serine starvation on mTORC1 activity and cell proliferation in ESCC cells.

Serine starvation inhibits NADPH synthesis and induces DNA oxidative damage

In addition to the oxidative PPP from glucose, NADPH is also derived from serine-driven folate cycle (Fig. S4A) [11]. To investigate the impact of serine deprivation on NADPH and GSH levels in ESCC cells, we measured the NADPH/$NADP^+$ and GSH/GSSG ratios. The result showed that serine starvation decreased the NADPH/$NADP^+$ and GSH/GSSG ratios in ESCC cells (Fig. 4A, B). Moreover, we measured the intermediates of PPP as PPP also produce NADPH. The results showed that no

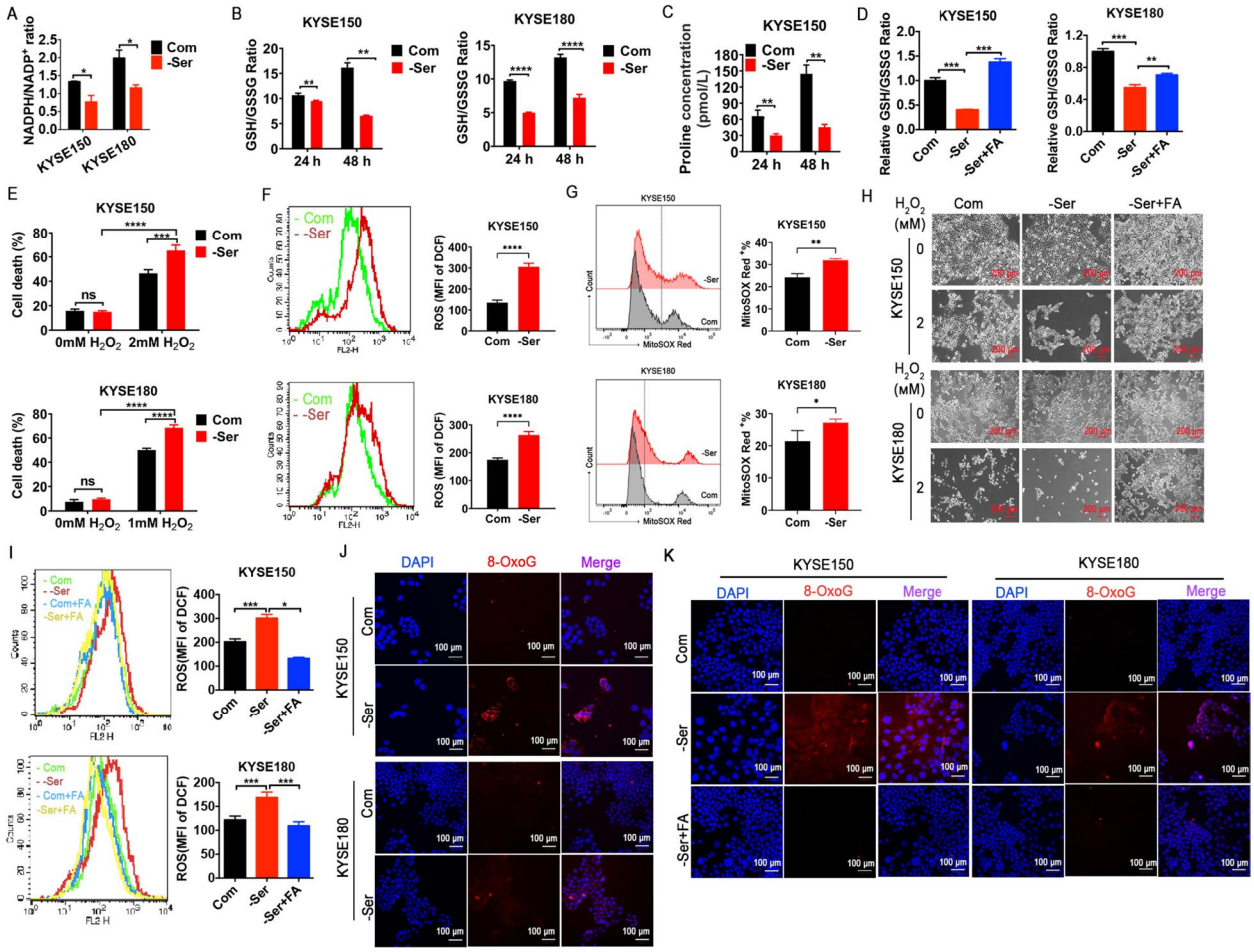

Fig. 4 Serine starvation inhibits NADPH synthesis and induces DNA oxidative damage. **A** The NADPH/$NADP^+$ ratio in ESCC cells cultured in Com or -Ser medium for 24 h. **B** The GSH/GSSG ratio in ESCC cells cultured in Com or -Ser medium for 24 and 48 h. **C** The proline level in KYSE150 cells cultured in Com or -Ser medium for 24 and 48 h was detected by HPLC. **D** The GSH/GSSG ratio of ESCC cells cultured in Com or -Ser medium with or without 1 mM FA for 24 h. **E** The mortality of ESCC cells cultured in Com or -Ser medium with or without H_2O_2 for 24 h was detected by using trypan blue staining. **F**, **G** The total and mitochondrial ROS levels of ESCC cells cultured in Com or -Ser medium for 48 h were measured by using 2′7′-DCFH-DA (**F**) and MitoSOX Red (**G**), respectively. **H** Representative images of ESCC cells cultured in Com or -Ser medium with the supplementation of 1 mM FA and/or 2 mM H_2O_2 for 24 h. Scale bar represents 200 μm. **I** The total ROS levels of ESCC cells cultured in Com or -Ser medium with or without 1 mM FA for 24 h. **J**, **K** Representative images of immunofluorescence assay of 8-OxoG in ESCC cells cultured in Com or -Ser medium with or without 1 mM FA for 48 h. DAPI was used to stain the nucleus. Scale bar represents 100 μm. Data are presented as mean ± SD. Unpaired two-sided Student's *t* test (**A**, **B**, **C**, **F** and **G**), and one-way ANOVA with Tukey's post hoc test (**D**, **E** and **I**). ns: no significance, $^*p < 0.05$, $^{**}p < 0.01$, $^{***}p < 0.001$, $^{****}p < 0.0001$

significant changes were observed in intermediates of PPP, such as 6-phosphogluconate and ribulose-5-phosphate, after serine deprivation (Fig. S4B), suggesting that decrease in NADPH/$NADP^+$ ratio caused by serine starvation is mainly dependent on the serine catabolism rather than PPP.

Since the hydrogen atom of NADPH derived from serine via folate cycle can be transferred into proline directly [11, 29], we further detected proline levels after serine starvation. The result showed that proline levels were decreased by 54% in KYSE150 cells, consisting with NADPH reduction after serine starvation (Fig. 4C). Meanwhile, the supplementation of 1 mM FA restored the reduction of GSH/GSSG ratio induced by serine starvation in ESCC cells (Fig. 4D). These results suggest that serine starvation significantly inhibits NADPH synthesis and disrupts the GSH/GSSG balance in ESCC cells.

The decreases of NADPH/$NADP^+$ and GSH/GSSG ratio hinted the impairment of antioxidant ability in ESCC cells after serine starvation. Thus, we examined the antioxidant ability of ESCC cells under hydrogen peroxide (H_2O_2)-induced oxidative stress after serine starvation for 24 h by measuring the cell mortality. The results showed that H_2O_2 treatment significantly increased the mortality of KYSE150 and KYSE180 cells in serine-deficient medium compared with control conditions (Fig. 4E). Moreover, we assessed the ROS levels and TCA cycle intermediates, as serine availability influences mitochondrial activity, which is crucial for redox homeostasis. Our findings revealed that both total and mitochondrial ROS levels were increased in ESCC cells after serine starvation (Fig. 4F, G). While the metabolites of TCA cycle, including pyruvate, α-ketoglutarate, succinate, malate, cis-aconitate, fumarate, and NADH/NAD^+ ratio, changed slightly after serine starvation (Fig. S4C). Interestingly, supplementation with 1 mM FA significantly rescued H_2O_2-induced oxidative stress (Fig. 4H) and decreased the intracellular ROS levels induced by serine starvation (Fig. 4I). These results suggest that serine starvation impairs redox homeostasis of ESCC cells, leading to increased vulnerability to oxidative damage.

Since excessive ROS can cause DNA oxidative damage by oxidizing guanine to 8-oxoguanine (8-OxoG), we evaluated the levels of 8-OxoG in ESCC cells after serine starvation using an immunofluorescence assay. The results showed an increase in 8-OxoG-positive cells after serine starvation for 24 h (Fig. 4J). This increase in 8-OxoG-positive cells was reduced by the supplementation of 1 mM FA (Fig. 4K). Taken together, these findings suggest that serine supports NADPH synthesis, which is crucial for maintaining redox homeostasis and preventing ROS-induced DNA damage in ESCC cells.

Serine starvation induces p53-p21 mediated G1 phase cell cycle arrest in ESCC cells

To gain further insight into the mechanism by which serine starvation induces DNA damage response, we applied mRNA sequencing (mRNA-seq) to explore the gene expression profiles in KYSE150 cells after serine starvation. Enrichment analysis of significantly changed genes using the GO and KEGG pathway databases revealed that the altered genes were closely associated with the cell cycle, nuclear division, nuclear chromosome segregation, p53 signaling pathway, and purine metabolism (Fig. 5A, B). We then performed qPCR assays to verify the representative genes identified through mRNA-seq, focusing on these involved in cell cycle regulation. The results showed that *TP53* and its downstream target genes, *CDKN1A* and *GADD45A*, were significantly upregulated following serine starvation (Fig. 5C). DNA damage triggers ATM to phosphorylate p53 at Ser15, promoting p53 accumulation and activating *CDKN1A* transcription [30]. Meanwhile, *CCNA2,* which is responsible for S phase progression, and *CCNB2,* which regulates G2/M transition, were significantly downregulated after serine starvation (Fig. 5C). Western blotting analysis confirmed that serine starvation upregulated the expression of p-p53 (Ser15) and p21 in both KYSE150 and KYSE180 cells, while moderately increased the total p53 level (Fig. 5D). To further confirm that G1 phase cell cycle arrest was induced by p53-p21, we silenced *P53* using two siRNAs numbered #1 and #2 (> 90% depletion compared with the control, Fig. 5E). As expected, p53 knockdown attenuated the upregulation of p21 induced by serine deprivation (Fig. 5E). These results suggest that serine starvation activates DNA damage response, characterized by activating p53-p21-mediated G1 phase cell cycle arrest in ESCC cells.

Since FA could rescue cell cycle arrest, DNA synthesis, and DNA oxidative damage induced by serine starvation, we measured the levels of cell cycle regulatory genes using qPCR in KYSE150 and KYSE180 cells cultured in serine-deficient medium supplemented with 1 mM FA. Consistently, the results showed that FA treatment restored the expression levels of these genes (Fig. 5F). Additionally, western blotting analysis revealed that FA attenuated the phosphorylation of p53 at Ser15 induced by serine starvation in both KYSE150 and KYSE180 cells (Fig. 5G). Collectively, the results suggest that serine starvation triggers p53-p21-mediated G1 phase cell cycle arrest via increasing DNA oxidative damage, and these effects can be mitigated by FA supplementation.

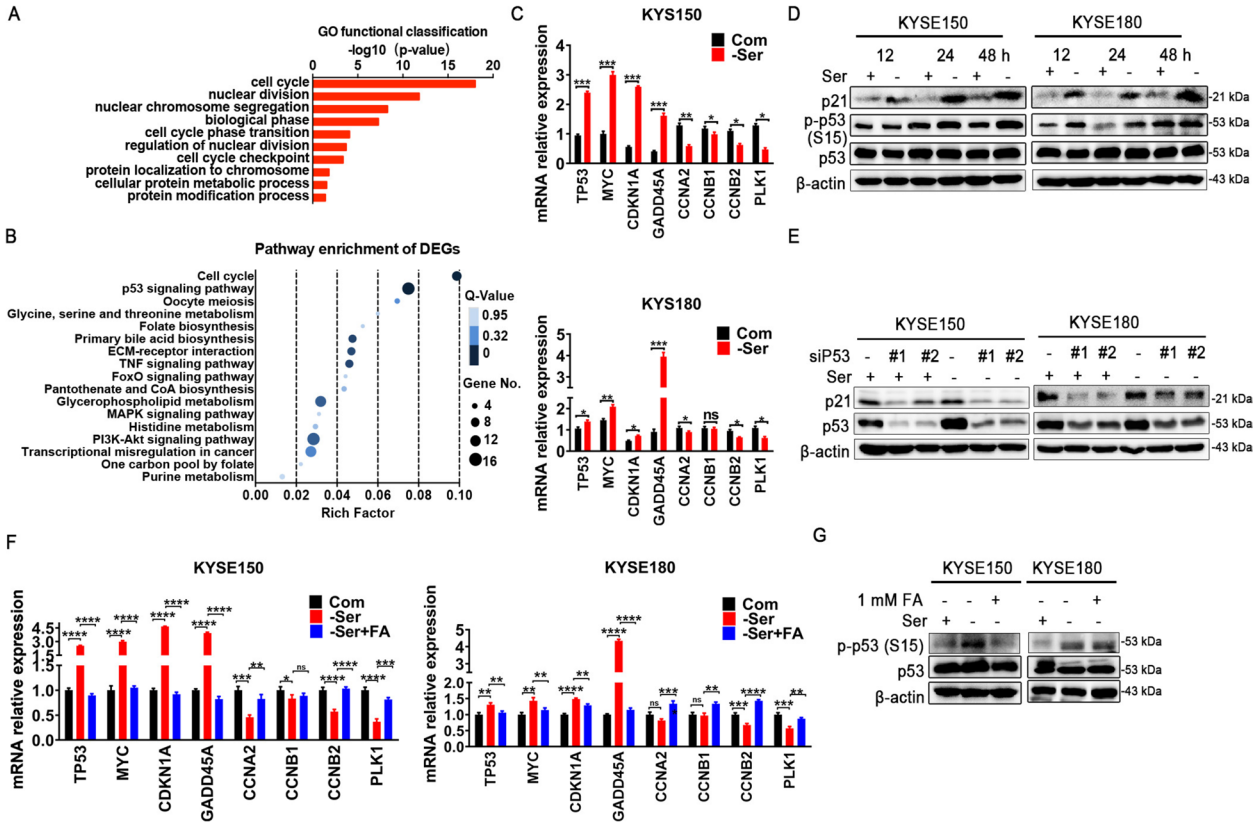

Fig. 5 Serine starvation induces p53-p21 mediated G1 phase cell cycle arrest in ESCC cells. **A** The difference genes of KYSE150 cells with serine starvation were analyzed by GO term. **B** The differentially expressed genes in KYSE150 cells with serine-starvation were enriched by KEGG. **C** The mRNA levels of cell cycle regulatory genes in ESCC cells grown in Com or -Ser medium for 24 h were detected by using qPCR. **D** The protein levels of p-p53 (Ser15) and p21 in ESCC cells grown in Com or -Ser medium for 24 h were detected by western blotting. β – actin was the loading control. **E** The protein levels of p53 and p21 in si*P53* ESCC cells grown in Com or -Ser medium for 24 h were detected by western blotting. β – actin was the loading control. **F** The mRNA levels of cell cycle regulatory genes in ESCC cells grown in Com or -Ser medium with the supplementary of 1 mM FA for 24 h were detected by using qPCR. **G** The protein levels of p-p53 (Ser15) and p53 in ESCC cells grown in Com or -Ser medium the supplementary of 1 mM FA for 24 h were detected by western blotting. β – actin was the loading control. Data are presented as mean ± SD. Unpaired two-sided Student's *t* test (**C**) and one-way ANOVA with Tukey's post hoc test (**F**). ns: no significance, *$p < 0.05$, **$p < 0.01$, ***$p < 0.001$, ****$p < 0.0001$

Serine starvation activates the metabolic enzymes of serine synthesis pathway (SSP) and increases endogenous serine synthesis

Given that serine acts as a natural ligand and allosteric activator of pyruvate kinase M2 [25, 31], serine starvation may channel the glycolytic intermediate 3-phosphoglycerate (3-PG) into SSP for serine synthesis. To investigate this effect, we monitored the serine and glycine levels in ESCC cells during serine starvation. Our results showed that serine and glycine levels were almost restored to normal at 24 h after serine deprivation (Fig. 6A, B). Consistently, serine starvation significantly promoted the upregulation of SSP enzymes, including phosphoglycerate dehydrogenase (*PHGDH*), *PSAT1*, and phosphoserine phosphatase (*PSPH*) (Fig. 6C, D and Fig. S5A), but did not affect SHMT2 (Fig. S5B). These results suggest that serine starvation activates the SSP for endogenous serine synthesis.

Transcription factor ATF4 transcriptionally activates serine biosynthetic genes in response to serine starvation in lung cancer cells [32]. Interestingly, we found that both the mRNA and protein levels of ATF4 were significantly upregulated in KYSE150 and KYSE180 cells under serine starvation (Fig. 6C, D). Data mining of the TCGA database revealed a positive correlation between *ATF4* expression and the expression of *PHGDH*, *PSAT1,* and *PSPH* in human ESCC tissues (Fig. 6E). Chromatin immunoprecipitation assays demonstrated that serine starvation induced remarkable recruitment of ATF4 to the promoters of the *PHGDH* and *PSAT1* genes but not to the *PSPH* promoter region in KYSE150 cells (Fig. 6F). Furthermore, the knockdown of *ATF4* using two siRNAs numbered #1 and #2

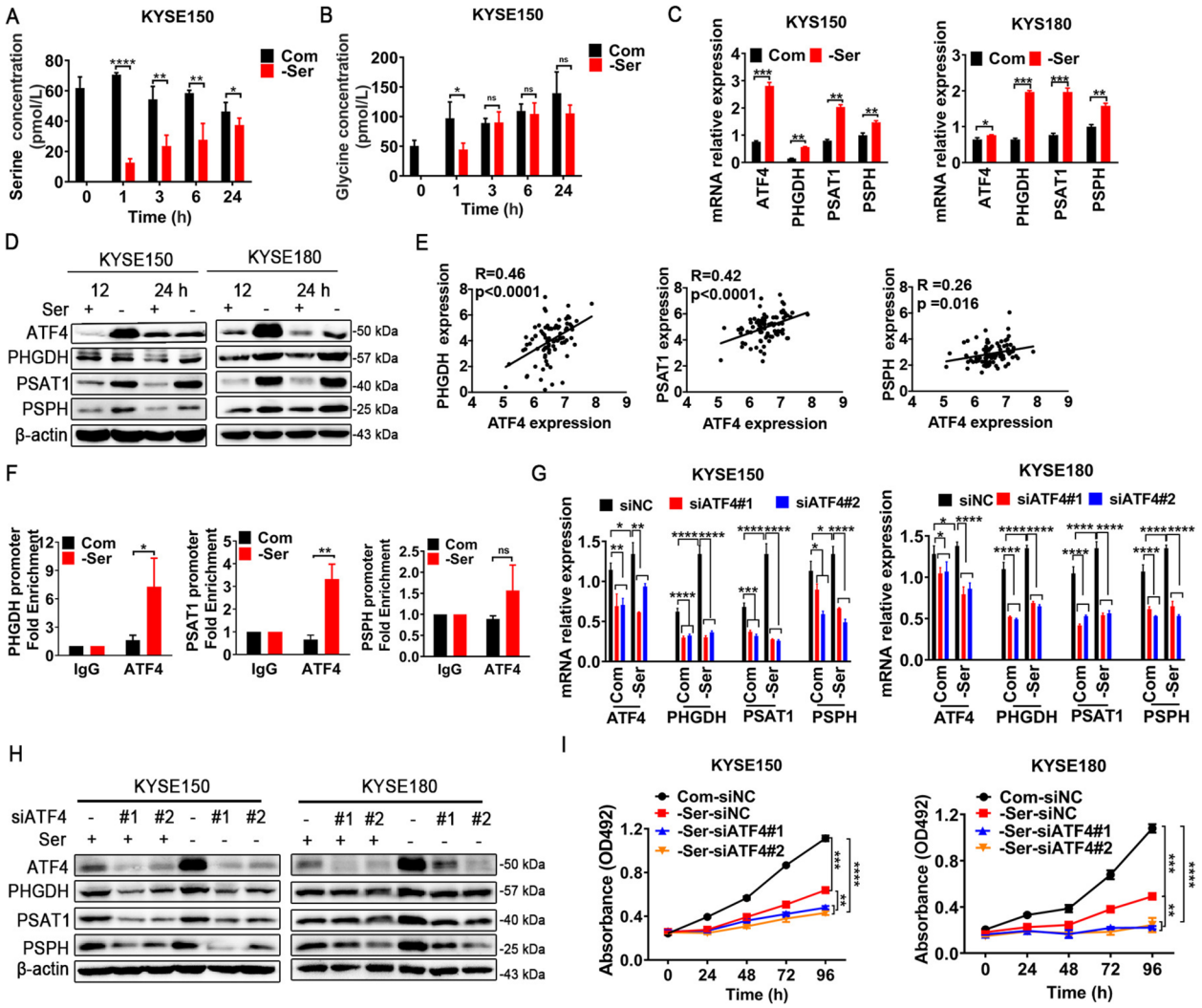

Fig. 6 Serine starvation activates metabolic enzymes of SSP and increases endogenous serine synthesis. **A**, **B** The concentration of intracellular serine (**A**) and glycine (**B**) in KYSE150 cells after serine starvation for indicated time were measured by HPLC, respectively. **C**, **D** The expression of *ATF4, PHGDH, PSAT1* and *PSPH* in ESCC cells after serine starvation for 12 and 24 h were detected by using qPCR (**C**) and western blotting (**D**). β – actin was the loading control. **E** The correlation of *ATF4* expression with *PHGDH*, *PSAT1*, and *PSPH* expression in human ESCC tissue samples were analyzed using TCGA database. Data are presented as Simple Linear Regression. **F** The binding of ATF4 to promoter of *PHGDH*, *PSAT1* and *PSPH* in KYSE150 cells grown in Com or -Ser medium for 24 h were measured by using ChIP-qPCR assay. IgG was used as the negative control. **G**, **H** The levels of *ATF4, PHGDH, PSAT1* and *PSPH* in *ATF4* knockdown ESCC cells grown in Com or -Ser medium for 12 h were detected by using qPCR (**G**) and western blotting (**H**). β – actin was the loading control. **I** Growth curves of ATF4 knockdown ESCC cells grown in Com or -Ser medium was determined by MTT assay. Data are presented as mean ± SD. Unpaired two-sided Student's *t* test (**A**, **B**, **C**, and **F**), one-way ANOVA with Tukey's post hoc test (**G**), and two-way ANOVA with Tukey's post hoc test (**I**). ns: no significance, $^{*}p < 0.05$, $^{**}p < 0.01$, $^{***}p < 0.001$, $^{****}p < 0.0001$

(> 50% depletion compared with the control) significantly attenuated the transcriptional upregulation of *PHGDH, PSAT1,* and *PSPH* genes induced by serine starvation (Fig. 6G, H) and completely inhibited cell proliferation (Fig. 6I). Collectively, our findings suggest that ATF4 mediates the transcriptional upregulation of *PHGDH* and *PSAT1* in ESCC cells after serine starvation, thereby promoting endogenous serine synthesis and supporting cell proliferation.

The combination of *PSAT1* knockdown and serine deprivation inhibits ESCC cell growth in vitro and in vivo

To investigate the key metabolic enzymes of the SSP that promote ESCC progression, we analyzed the gene expression of *PHGDH*, *PSAT1,* and *PSPH* in human ESCC tissues using the GEO and TCGA databases. Our analysis revealed that *PSAT1* and *PSPH* were significantly overexpressed in human ESCC tissues compared with normal esophageal tissues, whereas *PHGDH* expression showed

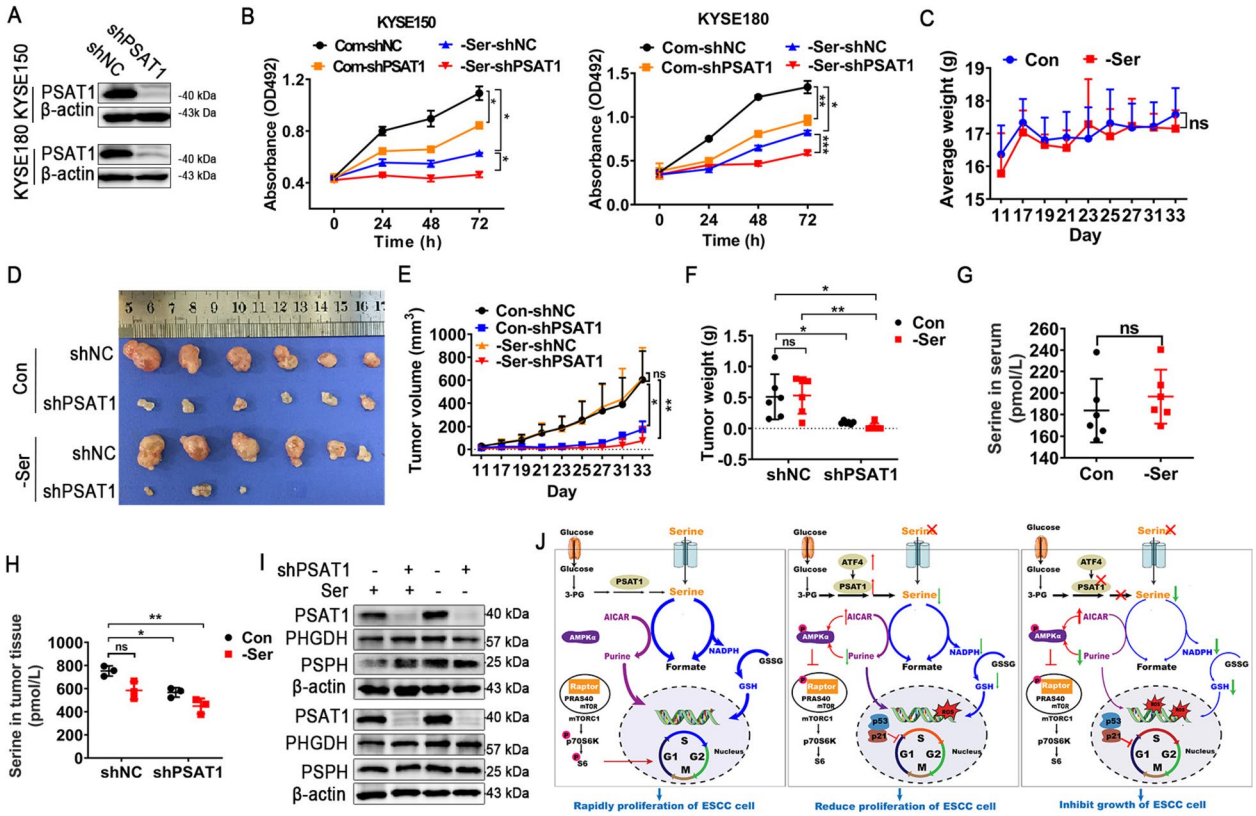

Fig. 7 The combination of *PSAT1* knockdown and serine deprivation inhibits ESCC cell growth in vitro and in vivo. **A** The verification of knockdown effect of *shPSAT1* by western blotting. β – actin was the loading control. **B** Growth curves of *PSAT1* knockdown ESCC cells grown in Com or -Ser medium was determined by MTT assay. **C**-**F** shNC or sh*PSAT1* KYSE150 cells were subcutaneously injected into nude mice ($n = 6$ per group). Mice were fed either control diet or diet lacking serine (-Ser) and sacrificed on day 33. The body weight of mice (**C**) and tumor volume (**E**) was measured at the indicated time intervals and calculated. At the end of treatment, the tumors were excised, photographed as indicated (**D**) and weighed (**F**). **G** Serum serine concentrations in mice described in C-F were measured by HPLC ($n = 6$ per group). (**H**) HPLC assessment of serine levels in tumors tissue described in C-F ($n = 3$ per group). **I** The protein levels of PSAT1, PHGDH and PSPH in tumor tissues described in C-F by western blotting. β – actin was the loading control. **J** Schematic diagram of serine supporting ESCC cell proliferation. Sufficient serine levels-mediated the synthesis of purine nucleotides and NADPH, which together maintained mTORC1 activity and redox homeostasis, promoting cell cycle progression and rapid ESCC cell proliferation. Exogenous serine starvation results in a reduction of purine nucleotide, inhibiting DNA synthesis, and a downregulation of NADPH, leading to increased cellular oxidative stress and DNA damage. These conditions stimulate p53-p21-mediated G1 phase cell cycle arrest. The AICAR and AMP/ATP ratio is significantly upregulated, leading to the activation of AMPKα. Activated AMPKα in turn phosphorylates Raptor, a subunit of mTORC1, which results in inhibition of mTORC1 activity and consequently reduces cell proliferation. Moreover, exogenous serine deprivation induces ATF4-mediated activation of SSP, allowing ESCC cells to adapt to serine starvation. Loss of serine (endogenous synthesis and exogenous starvation) completely inhibits the growth of ESCC cells. The combination of serine deprivation and *PSAT1* knockdown entirely inhibits the growth of ESCC cells. Data are presented as mean ± SD. Two-way ANOVA with Tukey's post hoc test (**B** and **E**), unpaired two-sided Student's *t* test (**C** and **G**), and one-way ANOVA with Tukey's post hoc test (**F** and **H**), and. ns: no significance, *$p < 0.05$, **$p < 0.01$, ***$p < 0.001$, ****$p < 0.0001$

no difference (Fig. S5C, D). qPCR and western blotting analysis further confirmed these findings (Fig. S5E, F). These results reveal that the upregulation of *PSAT1* is highly associated with ESCC progression.

We then silenced *PSAT1* using shRNA in KYSE150 and KYSE180 cells (> 90% depletion compared with the control, Fig. 7A) and further evaluated cell proliferation under serine-depleted conditions using MTT assay. The proliferation curves demonstrated that *PSAT1* knockdown inhibited ESCC cell proliferation (Fig. 7B). Moreover, the combination of *PSAT1* knockdown and serine deprivation completely halted ESCC cell survival in vitro (Fig. 7B).

To explore the antitumor efficacy of combination therapy in vivo, we used mice xenograft models with KYSE150 cells. Nude mice were subcutaneously injected with KYSE150 cells (*shPSAT1* right flank, shNC left flank), and fed either a control diet or serine-lacking diet. Unlike essential amino acids, the chronic deprivation of serine was well-tolerated in vivo, with no significant

changes in body weight observed (Fig. 7C). *PSAT1* knockdown alone resulted in a 71% reduction in tumors size compared to the shNC group (Fig. 7D-F). However, serine-lacking diet had no significant effect on the growth of tumors arising from KYSE150 shNC cells (Fig. 7D-F). The combination of *PSAT1* knockdown and serine-lacking diet strongly inhibited tumor growth (Fig. 7D-F). These results showed that PSAT1 plays a crucial role in sustaining ESCC tumor growth in vivo.

We then measured the serine concentration in the serum of mice and tumor tissues using HPLC at the endpoint of the studies. The results showed that the serine-lacking diet alone resulted in a slight but no significant decrease in serine levels in serum and tumor tissues (Fig. 7G, H). However, the combination of *PSAT1* knockdown and serine deprivation obviously decreased serine level in tumor tissues (Fig. 7H). Consistently, serine-lacking diet significantly upregulated PSAT1 expression, which helped maintain the serine level in xenograft tumors (Fig. 7I). Given that glycine could be converted to serine through SHMT1/2, we further utilized serine/glycine-lacking (-SG) diet to intervene tumor growth. The result showed that -SG diet had no effect on tumor growth (Fig. S5G). Taken together, these results demonstrate that neither the -Ser nor the -SG diets alone significantly affected tumor growth, and the combination of *PSAT1* knockdown and serine deprivation strongly inhibits the growth of ESCC tumors in vivo.

Discussion

Previous studies have highlighted the importance of serine in maintaining cancer cell proliferation through various pathways, including nucleotide synthesis [33], redox balance [29], methionine cycle [34], and lipid metabolism [35]. However, it remains largely unknown how serine metabolism contributes to ESCC cell proliferation and the underlying mechanism. In the current study, we found that serine supported the rapid proliferation of ESCC cells. Mechanism study revealed that serine maintains the rapid proliferation and redox balance of ESCC cells by participating in purine nucleotide and NADPH synthesis, which subsequently regulates the AMPKα/mTORC1 signaling pathway and p53-p21-mediated G1 phase cell cycle. Serine deprivation in combination with PSAT1 inhibition exhibited significant inhibition of ESCC tumor growth in vitro and in vivo. Collectively, our study reveals the important role of serine in ESCC progression and provides a potential therapeutic strategy for ESCC.

The incorporation of serine-derived 10-formyl-THF is required at two points during the de novo purine nucleotides synthesis. Recent studies have reported that inhibition of one-carbon metabolism through serine starvation or genetic deletion of enzymes involved in the SSP decreases purine nucleotide levels [29, 36–38]. To evaluate the effect of serine-derived 10-formyl-THF on cellular processes under serine-depleted conditions, we employed FA, a one-carbon donor, as a substitute for 10-formyl-THF. Our results showed that the FA restored cellular processes impaired by serine starvation, including: cell proliferation, G1 phase cell cycle arrest, DNA synthesis, DNA oxidative damage and mTORC1 signaling pathway. Based on these findings, we hypothesize that serine regulates these cellular processes primarily through its role in providing 10-formyl-THF. Besides serine, glycine which can be endogenously synthesized from serine by SHMT1/2 or exogenously obtained outside the cell is an important substrate for de novo purine biosynthesis, particularly through the GART reaction [39]. In our study, we found that serine starvation only temporarily decreased glycine level, and glycine level almost returned to normal 3 h after serine starvation. We speculate that ESCC cells can obtain the exogenous glycine from medium when endogenous glycine synthesis is impaired by the depletion of serine. Therefore, we do not particularly highlight the role of glycine in de novo purine synthesis in our study. Thus, there are broader implications of serine depletion on metabolic reprogramming through alternative pathways in ESCC cells. For example, serine is an important source of fatty acid synthesis, and our mRNA-seq results found that serine starvation induced gene changes in glycerophospholipid metabolism in ESCC cells [40]. These alternative pathways remain an area worthy of further exploration to fully understand the metabolic adaptability of ESCC cells under serine-limited conditions.

Serine-derived one-carbon units also contributes to the production of NADPH, a key functional metabolite that provides reducing power for redox reactions [11]. However, the effect of serine-regulated NADPH on cell redox homeostasis has rarely been studied, especially in ESCC. In this study, we found that NADPH regulated through serine plays an important role in clearing ROS and sustaining redox homeostasis in ESCC cells. Furthermore, serine starvation-induced decreases in NADPH levels led to DNA oxidative damage and a p53-p21-meditaed DNA damage response. While the importance of serine metabolism in proliferating cells has traditionally been attributed to nucleotide synthesis, our study revealed that NADPH derived from serine catabolism is also vital for maintaining the cell cycle and proliferation of ESCC cells. Besides NADPH, NADH also play an important role in maintaining cellular redox homeostasis, and de novo serine synthesis produce NADH when PHGDH converts the glycolytic intermediate 3-PG to phosphohydroxypyruvate (p-Pyr), which is the first and rate limiting step of serine

synthesis [41]. Our result showed that serine starvation slightly reduced the NADH production, which may contribute to ROS production induced by serine starvation.

AMPK is an evolutionarily conserved serine/threonine kinase that plays a central role in maintaining cellular metabolic balance [42] and responding to disruptions in cellular energy by suppressing mTORC1 signaling and inducting fatty acid oxidation [43]. AMPK is activated by various conditions, including but not limited to energy disruption, ROS-induced DNA damage [44], and AICAR activation [45]. In our study, we observed that serine starvation activates AMPK through the accumulation of AICAR and an increased AMP/ATP ratio. The activation of AMPK promotes p53 activity through phosphorylation at Ser15 under glucose starvation conditions, which regulates the cell cycle [46]. We also found that serine starvation led to the upregulation of p-p53 (Ser15), which is responsible for the DNA damage response and mediates G1-phase arrest in cells. Whether the upregulation of p-p53 (Ser15) was directly mediated by AMPK activation requires further verification.

mTORC1 is a master regulator of cell growth and serves as a key molecular sensor for nutrient availability, including amino acids [47]. Essential amino acids leucine and arginine mediate the activation of mTORC1 by the Rag A/B complex [23]. The nonessential amino acid serine can also maintain mTORC1 activation. Deprivation of exogenous serine has been shown to inhibit the phosphorylation of p70S6K and S6, which are downstream effectors of mTORC1 in human lung cancer cells [25]. However, it is not clear how serine contributes to mTORC1 activity. Maddocks et al. found that serine starvation inhibited mTORC1 activity in a p53-independent manner [9]. In our study, we confirmed that the inhibitory effect of serine starvation on mTORC1 signaling is mediated by AMPKα directly phosphorylating Raptor at Ser792. This finding illustrated the mechanism by which serine starvation contributes to mTORC1 inhibition.

Although serine deprivation effectively inhibited ESCC cell proliferation in vitro, a serine-lacking (-Ser) diet or serine/glycine-lacking (-SG) alone did not inhibit tumor growth in vivo. This result is similar with previous studies showing that -SG diet did not affect tumor growth in various models in vivo, including HCT116, DLD-1 [37], MC38 [48], spontaneous pancreatic cancer model [26], and primary breast cancer cells [49]. The activation of SSP appears to be the primary reason for this outcome. These results were consistent with our observations that serine starvation significantly promoted ATF4-mediated SSP activation. Thus, serine deprivation in combination with *PSAT1* knockdown is an effective strategy for ESCC treatment as our results showed that this combination significantly inhibited ESCC tumor growth in vivo.

In summary, the current study demonstrated that serine promotes ESCC cell proliferation by maintaining DNA synthesis and redox homeostasis and revealed a novel mechanism by which serine maintains mTORC1 activation (Fig. 7J). These findings provide a reliable theoretical basis for developing inhibitors that target serine metabolism as a potential treatment strategy for ESCC.

Supplementary Information

The online version contains supplementary material available at https://doi.org/10.1186/s40170-025-00376-4.

Supplementary Material 1.

Supplementary Material 2.

Supplementary Material 3.

Supplementary Material 4.

Acknowledgements
We thank the Analytical & Testing Center (Sichuan University, Chengdu, China) for providing technical support of metabolomics.

Authors' contributions
YLZ designed the experiments. HJ, JW, ZLL, MY, XYQ, YL, CQL, CL and LW performed the experiments. PCD, LXL and XBC provided clinical samples and analysis suggestions. YLZ and HJ analyzed the data. YLZ and HJ wrote the manuscript. All authors read and approved the final manuscript.

Funding
This work was supported by Project of the National Natural Science Foundation of China (82272716), and 1·3·5 Project for Disciplines of Excellence, West China Hospital, Sichuan University (ZYGD23011).

Data availability
No datasets were generated or analysed during the current study.

Declarations

Ethics approval and consent to participate
All animal experiments were approved by the Institutional Animal Care and Treatment Committee of Sichuan University in China (Permit Number: 20181025), and complied to National Institutes of Health guide for the care and use of laboratory animals.

Consent for publication
The manuscript is approved by all authors for publication.

Competing interests
The authors declare no competing interests.

Received: 25 March 2024 Accepted: 24 January 2025
Published online: 13 February 2025

References

1. Bray F, Laversanne M, Sung H, Ferlay J, Siegel RL, Soerjomataram I, et al. Global cancer statistics 2022: GLOBOCAN estimates of incidence and mortality worldwide for 36 cancers in 185 countries. CA Cancer J Clin. 2024;74(3):229–63.
2. Lagergren J, Smyth E, Cunningham D, Lagergren P. Oesophageal cancer. Lancet. 2017;390(10110):2383–96.

3. Hosios AM, Hecht VC, Danai LV, Johnson MO, Rathmell JC, Steinhauser ML, et al. Amino acids rather than glucose account for the majority of cell mass in proliferating mammalian cells. Dev Cell. 2016;36(5):540–9.
4. Locasale JW. Serine, glycine and one-carbon units: cancer metabolism in full circle. Nat Rev Cancer. 2013;13(8):572–83.
5. Jain M, Nilsson R, Sharma S, Madhusudhan N, Kitami T, Souza AL, et al. Metabolite profiling identifies a key role for glycine in rapid cancer cell proliferation. Science. 2012;336(6084):1040–4.
6. Labuschagne CF, van den Broek NJ, Mackay GM, Vousden KH, Maddocks OD. Serine, but not glycine, supports one-carbon metabolism and proliferation of cancer cells. Cell Rep. 2014;7(4):1248–58.
7. Possemato R, Marks KM, Shaul YD, Pacold ME, Kim D, Birsoy K, et al. Functional genomics reveal that the serine synthesis pathway is essential in breast cancer. Nature. 2011;476(7360):346–50.
8. Locasale JW, Grassian AR, Melman T, Lyssiotis CA, Mattaini KR, Bass AJ, et al. Phosphoglycerate dehydrogenase diverts glycolytic flux and contributes to oncogenesis. Nat Genet. 2011;43(9):869–74.
9. Maddocks OD, Berkers CR, Mason SM, Zheng L, Blyth K, Gottlieb E, et al. Serine starvation induces stress and p53-dependent metabolic remodelling in cancer cells. Nature. 2013;493(7433):542–6.
10. Son J, Lyssiotis CA, Ying H, Wang X, Hua S, Ligorio M, et al. Glutamine supports pancreatic cancer growth through a KRAS-regulated metabolic pathway. Nature. 2013;496(7443):101–5.
11. Fan J, Ye J, Kamphorst JJ, Shlomi T, Thompson CB, Rabinowitz JD. Quantitative flux analysis reveals folate-dependent NADPH production. Nature. 2014;510(7504):298–302.
12. Laplante M, Sabatini DM. mTOR signaling in growth control and disease. Cell. 2012;149(2):274–93.
13. Jewell JL, Guan KL. Nutrient signaling to mTOR and cell growth. Trends Biochem Sci. 2013;38(5):233–42.
14. Shimobayashi M, Hall MN. Making new contacts: the mTOR network in metabolism and signalling crosstalk. Nat Rev Mol Cell Biol. 2014;15(3):155–62.
15. Aspuria PJ, Tamanoi F. The Rheb family of GTP-binding proteins. Cell Signal. 2004;16(10):1105–12.
16. Gwinn DM, Shackelford DB, Egan DF, Mihaylova MM, Mery A, Vasquez DS, et al. AMPK phosphorylation of raptor mediates a metabolic checkpoint. Mol Cell. 2008;30(2):214–26.
17. Sancak Y, Bar-Peled L, Zoncu R, Markhard AL, Nada S, Sabatini DM. Ragulator-Rag complex targets mTORC1 to the lysosomal surface and is necessary for its activation by amino acids. Cell. 2010;141(2):290–303.
18. Shimobayashi M, Hall MN. Multiple amino acid sensing inputs to mTORC1. Cell Res. 2016;26(1):7–20.
19. Nicklin P, Bergman P, Zhang B, Triantafellow E, Wang H, Nyfeler B, et al. Bidirectional transport of amino acids regulates mTOR and autophagy. Cell. 2009;136(3):521–34.
20. Hara K, Yonezawa K, Weng QP, Kozlowski MT, Belham C, Avruch J. Amino acid sufficiency and mTOR regulate p70 S6 kinase and eIF-4E BP1 through a common effector mechanism. J Biol Chem. 1998;273(23):14484–94.
21. Wang S, Tsun ZY, Wolfson RL, Shen K, Wyant GA, Plovanich ME, et al. Metabolism. Lysosomal amino acid transporter SLC38A9 signals arginine sufficiency to mTORC1. Science. 2015;347(6218):188–94.
22. Wolfson RL, Chantranupong L, Saxton RA, Shen K, Scaria SM, Cantor JR, et al. Sestrin2 is a leucine sensor for the mTORC1 pathway. Science. 2016;351(6268):43–8.
23. Wang YP, Lei QY. Metabolite sensing and signaling in cell metabolism. Signal Transduct Target Ther. 2018;3:30.
24. Ye J, Palm W, Peng M, King B, Lindsten T, Li MO, et al. GCN2 sustains mTORC1 suppression upon amino acid deprivation by inducing Sestrin2. Genes Dev. 2015;29(22):2331–6.
25. Ye J, Mancuso A, Tong X, Ward PS, Fan J, Rabinowitz JD, et al. Pyruvate kinase M2 promotes de novo serine synthesis to sustain mTORC1 activity and cell proliferation. Proc Natl Acad Sci U S A. 2012;109(18):6904–9.
26. Maddocks ODK, Athineos D, Cheung EC, Lee P, Zhang T, van den Broek NJF, et al. Modulating the therapeutic response of tumours to dietary serine and glycine starvation. Nature. 2017;544(7650):372–6.
27. Tibbetts AS, Appling DR. Compartmentalization of Mammalian folate-mediated one-carbon metabolism. Annu Rev Nutr. 2010;30:57–81.
28. Maddocks OD, Labuschagne CF, Adams PD, Vousden KH. Serine metabolism supports the methionine cycle and DNA/RNA methylation through De Novo ATP synthesis in cancer cells. Mol Cell. 2016;61(2):210–21.
29. Ducker GS, Chen L, Morscher RJ, Ghergurovich JM, Esposito M, Teng X, et al. Reversal of cytosolic one-carbon flux compensates for loss of the mitochondrial folate pathway. Cell Metab. 2016;23(6):1140–53.
30. Ma Y, Vassetzky Y, Dokudovskaya S. mTORC1 pathway in DNA damage response. Biochim Biophys Acta Mol Cell Res. 2018;1865(9):1293–311.
31. Chaneton B, Hillmann P, Zheng L, Martin ACL, Maddocks ODK, Chokkathukalam A, et al. Serine is a natural ligand and allosteric activator of pyruvate kinase M2. Nature. 2012;491(7424):458–62.
32. DeNicola GM, Chen PH, Mullarky E, Sudderth JA, Hu Z, Wu D, et al. NRF2 regulates serine biosynthesis in non-small cell lung cancer. Nat Genet. 2015;47(12):1475–81.
33. Ducker GS, Rabinowitz JD. One-carbon metabolism in health and disease. Cell Metab. 2017;25(1):27–42.
34. Gao X, Locasale JW, Reid MA. Serine and methionine metabolism: vulnerabilities in lethal prostate cancer. Cancer Cell. 2019;35(3):339–41.
35. Gao X, Lee K, Reid MA, Sanderson SM, Qiu C, Li S, et al. Serine availability influences mitochondrial dynamics and function through lipid metabolism. Cell Rep. 2018;22(13):3507–20.
36. Ma EH, Bantug G, Griss T, Condotta S, Johnson RM, Samborska B, et al. Serine is an essential metabolite for effector T cell expansion. Cell Metab. 2017;25(2):345–57.
37. Tajan M, Hennequart M, Cheung EC, Zani F, Hock AK, Legrave N, et al. Serine synthesis pathway inhibition cooperates with dietary serine and glycine limitation for cancer therapy. Nat Commun. 2021;12(1):366.
38. Yu W, Wang Z, Zhang K, Chi Z, Xu T, Jiang D, et al. One-carbon metabolism supports S-adenosylmethionine and histone methylation to drive inflammatory macrophages. Mol Cell. 2019;75(6):1147-60 e5.
39. Ali ES, Ben-Sahra I. Regulation of nucleotide metabolism in cancers and immune disorders. Trends Cell Biol. 2023;33(11):950–66.
40. Hirabayashi Y, Furuya S. Roles of l-serine and sphingolipid synthesis in brain development and neuronal survival. Prog Lipid Res. 2008;47(3):188–203.
41. Wang C, Chen Q, Chen S, Fan L, Gan Z, Zhao M, et al. Serine synthesis sustains macrophage IL-1β production via NAD+-dependent protein acetylation. Mol Cell. 2024;84(4):744-59.e6.
42. Rabinovitch RC, Samborska B, Faubert B, Ma EH, Gravel SP, Andrzejewski S, et al. AMPK maintains cellular metabolic homeostasis through regulation of mitochondrial reactive oxygen species. Cell Rep. 2017;21(1):1–9.
43. Zhang D, Tang Z, Huang H, Zhou G, Cui C, Weng Y, et al. Metabolic regulation of gene expression by histone lactylation. Nature. 2019;574(7779):575–80.
44. Rodríguez-Vargas JM, Ruiz-Magaña MJ, Ruiz-Ruiz C, Majuelos-Melguizo J, Peralta-Leal A, Rodríguez MI, et al. ROS-induced DNA damage and PARP-1 are required for optimal induction of starvation-induced autophagy. Cell Res. 2012;22(7):1181–98.
45. Zang M, Liu S, Jing F, Yu C, Gao L, Qin Y, et al. AICAR-induced activation of AMPK inhibits TSH/SREBP-2/HMGCR pathway in liver. PLoS ONE. 2015;10(5):e0124951.
46. Jones RG, Plas DR, Kubek S, Buzzai M, Mu J, Xu Y, et al. AMP-activated protein kinase induces a p53-dependent metabolic checkpoint. Mol Cell. 2005;18(3):283–93.
47. Park Y, Reyna-Neyra A, Philippe L, Thoreen CC. mTORC1 balances cellular amino acid supply with demand for protein synthesis through post-transcriptional control of ATF4. Cell Rep. 2017;19(6):1083–90.
48. Gravel SP, Hulea L, Toban N, Birman E, Blouin MJ, Zakikhani M, et al. Serine deprivation enhances antineoplastic activity of biguanides. Cancer Res. 2014;74(24):7521–33.
49. Sullivan MR, Mattaini KR, Dennstedt EA, Nguyen AA, Sivanand S, Reilly MF, et al. Increased serine synthesis provides an advantage for tumors arising in tissues where serine levels are limiting. Cell Metab. 2019;29(6):1410-21.e4.

Publisher's Note